Research Square

Preprints are preliminary reports that have not undergone peer review.
They should not be considered conclusive, used to inform clinical practice,
or referenced by the media as validated information.

Sustainable Waterborne Polyurethanes with Improved Self-Healing and Performance Using Bio-Derived Vanillin and Olive Oil Polyols

Ali Reza Banan

bananjahromi@yahoo.com

Imam Hossein University

Research Article

Keywords: Waterborne polyurethane, Olive Oil-Derived Polyols, Self-Healing Polymers, Polyurethane Coatings, Dynamic imine bond, Vanillin diol

Posted Date: March 25th, 2026

DOI: https://doi.org/10.21203/rs.3.rs-8479000/v1

License: This work is licensed under a Creative Commons Attribution 4.0 International License.
Read Full License

Additional Declarations: No competing interests reported.

Abstract

This study introduces a new waterborne polyurethane (WPU) system that incorporates a vanillin-derived diol with dynamic Schiff base linkages, enabling reversible covalent interactions within the polymer matrix. Vanillin, an economical, bio-sourced molecule, was utilized to synthesize this functional diol, which was included as a chain extender with olive oil-derived polyols (OOP) and isophorone diisocyanate (IPDI). The incorporation of Schiff base chemistry into the system imparts self-healing and reprocessability properties to the material while also enhancing its mechanical integrity. A Design of Experiments (DoE) methodology was employed to optimize the formulation, concentrating on key factors including dimethylolpropionic acid (DMPA), vanillin diol (VAN-OH), and olive oil polyols. The optimized WPU-VAN-OH formulation demonstrated a tensile strength of 9.2 MPa and showed exceptional thermal stability, with a degradation onset temperature of 354°C. The WPU-VAN-OH formulation demonstrated remarkable self-healing capabilities, with full restoration of surface scratches within 30 minutes at 70°C. The synthetic WPU films were evaluated for their structural, thermal, and mechanical properties using NMR, FT-IR, SEM, and mechanical tests. The findings demonstrate the appropriateness of the WPU-VAN-OH system for applications necessitating durable, self-repairing, and eco-friendly materials.

Introduction

The rising demand for resources and energy comes from an unsustainable dependence on fossil fuels, fueled by global population growth and continuous technological advancement.[1–3] This increasing dependence raises significant concerns regarding resource depletion and environmental degradation, including pollution and greenhouse gas emissions.[4, 5] Most of the polymers used in everyday life are made from non-renewable petrochemical feedstocks, which are limited and have a substantial negative impact on the environment.[6, 7] As a result, there is an urgent need to develop sustainable alternatives that meet both performance requirements and environmental standards.[8] In response to these challenges, researchers and industries are increasingly turning to biomass-derived products as promising alternatives.[9] Natural renewable resources, such as starch, cellulose, chitosan, and vegetable oils, have garnered significant interest owing to their abundance, renewability, biodegradability, and comparatively low cost.[10, 11] These attributes render them appealing alternatives to traditional petroleum-derived materials in multiple industries.[12] Vegetable oils are distinguished among bio-based feedstocks for their chemical versatility and extensive availability. Their molecular structure, abundant in triglycerides with ester linkages and unsaturated carbon-carbon double bonds, offers extensive potential for chemical modification.[13] These functional groups facilitate the synthesis of customized monomers and polymers, rendering vegetable oils optimal precursors for the development of high-performance, environmentally sustainable products.[14]

With the increasing attention to developing environmentally friendly alternatives, polyurethane (PU) chemistry is playing an increasingly important role in achieving sustainability.[15] Polyurethanes, which are

widely used in coatings, adhesives, foams, textiles, and biomedical applications due to their excellent mechanical properties, high durability, and formulation flexibility, are highly flexible synthetic polymers.[16] However, traditional polyurethanes are usually dependent on solvent-based systems that generate hazardous volatile organic compounds (VOCs), thus posing a threat to human health and the environment.[17] waterborne polyurethanes (WPU) are considered as a green alternative to these problems.[18] Despite their low viscosity, WPU offer many advantages, including increased processability, reduced VOC emissions, and reduced flammability.[19] These features are fully in line with the growing consumer demand for environmentally friendly products, as well as the need to implement stricter environmental regulations.[20] One of the main goals in the development of WPU is to replace petroleum-derived components, such as polyols and chain extenders, with bio-based alternatives.[21, 22] Vegetable oils are an ideal choice for this purpose due to their natural renewable nature and high chemical compatibility.[23] By exploiting the reactive double bonds present in unsaturated fatty acids, functional derivatives such as hydroxylated polyols or epoxidized oils can be produced, which are easily incorporated into WPU formulations.[24]

Olive oil (OO), a plant-derived oil abundant in triglycerides mainly consisting of oleic acid presents distinct possibilities in this regard.[25, 26] Thanks to its high level of unsaturation, olive oil offers multiple reactive sites that can easily undergo specific chemical transformations.[27] Common approaches include epoxidation followed by ring-opening reactions to create hydroxyl-functional molecules, as well as thiol–ene click chemistry, which allows for the efficient attachment of thiol groups to carbon–carbon double bonds.[28] These developments allow the production of tailored polymers that greatly improve the WPU system performance.[29] Although they still meet industrial needs for strength, flexibility, and durability, researchers want to reduce reliance on fossil fuels in polymer design by including bio-based components.[30] This approach supports sustainable chemistry, so tying environmental awareness to the development of high-performance materials. It marks a more general trend in research towards more ecologically friendly solutions.[31]

Polyurethanes, due to their rigid and permanent structure, have traditionally been considered non-recyclable, contributing to long-term environmental waste.[32] Incorporating reversible covalent bonds that enable recyclability, reprocessing, and self-healing properties, covalent adaptable networks (CANs) have evolved as a sustainable alternative.[33–35] Among the several dynamic chemistries, imine exchange between amines and aldehydes is unique in efficiency and adaptability.[36] Within this framework, vanillin a monomer obtained from lignin, has emerged as a subject of growing interest owing to its sustainable origin and multifunctional chemical properties. Its special chemical composition, which combines hydroxyl with aldehyde groups, makes it an excellent candidate for the formulation of environmentally friendly, high-performance polyurethanes.[37] Notwithstanding present difficulties, including synthesis complexity and mechanical limitations, vanillin-based systems show great potential for the development of next-generation sustainable and functional polymer materials.[38]

This study synthesizes a new diol derived from vanillin with terminal Schiff base couplings to enhance reversible covalent contacts inside a polyurethane matrix. We developed a WPU system that integrates the characteristics of vanillin, a cost-effective, bio-derived aromatic compound, with isophorone diisocyanate (IPDI) and olive oil-derived polyols (OOP). The integration of Schiff base chemistry into the polymer backbone facilitates self-healing and reprocessability while also enhancing mechanical strength and thermal resistance. A rigorous Design of Experiments (DoE) methodology was employed to refine the formulation. The optimized WPU-VAN-OH formulation demonstrated superior tensile strength, improved thermal stability, and significant self-healing properties under mild heating settings. The following sections discuss the synthesis strategy, characterization methods, and comprehensive evaluation of the material's properties.

Experimental

2.1. Materials

Commercial-grade olive oil (OO) was procured from Luyeh Food Industries Company, in Rudbar, Gilan Province, Iran. Isophorone diisocyanate (IPDI, 99% purity) was supplied by Rongrong Chemical Ltd. Vanillin (VAN, 98%) and ethanolamine (EDA, 99%) were obtained from Sigma-Aldrich and used without further purification. Dimethylolpropionic acid (DMPA, 98%), triethylamine (TEA, 98%), and dibutyltin dilaurate (DBTDL, 98%) were purchased from Merck. Analytical-grade ethanol and ethylene glycol (both with purity ≥ 99.8%) were also obtained from Merck. Throughout all experimental procedures, deionized water was used to ensure high reproducibility and minimize contamination. All chemicals were of analytical or reagent grade and used without any additional purification unless otherwise specified.

2.2. Synthesis of Vanillin Diol (VAN-OH)

To synthesize VAN-OH, 5.0 g (32 mmol) of vanillin was first dissolved in 5 mL of absolute ethanol and transferred into a 100 mL three-necked round-bottom flask equipped with a reflux condenser and a magnetic stirrer.[39, 40] Subsequently, ethanolamine (1.95 g, 32 mmol) was added dropwise under continuous stirring. Upon addition, a yellow precipitate began to form immediately, indicating the initiation of the imine formation reaction. The reaction mixture was gradually heated to 55°C and maintained under reflux conditions for 8 hours to ensure complete conversion. During the reaction, the color of the solution gradually changed from pale yellow to deep red, confirming the progression of the reaction toward the formation of the target compound. After completion, the reaction mixture was subjected to vacuum drying at 70°C for 24 hours until a constant weight was achieved. The final product was obtained as a red, viscous liquid and was designated as VAN-OH. The isolated yield was 6.4 g, 92.62%.

2.3. Synthesis of Olive Oil-Based Polyols

The preparation of polyols from olive oil involved a two-step process: epoxidation of the double bonds followed by an acid-catalyzed ring-opening reaction to generate hydroxyl-functional compounds (as

illustrated in Fig. 1). The epoxidation reaction was carried out using a modified version of a previously published method.[41–43] In this step, hydrogen peroxide (30 wt%) and formic acid (88 wt%) were used as oxidizing agents under mild conditions. In a typical procedure, 250 g of refined olive oil was introduced into a round-bottom flask equipped with a mechanical stirrer, followed by the addition of 100 g of hydrogen peroxide and 38 g of formic acid. The mixture was stirred continuously in a water bath maintained at 25°C for a period of 21 hours. Following completion of the reaction, the product was purified by extraction with ethyl acetate, followed by washing with an aqueous sodium chloride solution. Residual acidity was neutralized using sodium bicarbonate until a neutral pH was achieved. The organic phase was then dried over anhydrous magnesium sulfate, filtered under vacuum, and subjected to rotary evaporation at 60°C for 1 hour. Finally, the epoxidized olive oil was dried overnight in a convection oven at 50°C.

For the ring-opening reaction, hydrochloric acid (37.3%, 58.7 g, 0.600 mol) was dissolved in 250 mL of acetone in a 500 mL flask. Epoxidized olive oil (100 g, corresponding to 0.280 mol of oxirane groups) was slowly added dropwise to the acidic solution under vigorous stirring. During the addition, which lasted approximately 15 minutes, the temperature of the reaction mixture rose to around 45°C. Stirring was continued for an additional hour to ensure complete ring opening. After the reaction, 300 mL of ethyl acetate and 100 mL of deionized water were added to the mixture, and the organic and aqueous layers were separated. The organic layer was washed repeatedly with water until the washings reached a neutral pH. It was then dried over magnesium sulfate, filtered, and concentrated under reduced pressure. A yellow viscous liquid (113 g) was obtained as the final polyol product. Purification of the synthesized olive oil-based polyol was carried out by extraction with ethyl acetate and subsequent washing with an aqueous sodium chloride solution. Subsequently, it was vacuum-filtered, rotary-evaporated at 50°C for 1 hour, and dried in a 60°C oven overnight to remove residual solvents and moisture prior to characterization and use in polyurethane synthesis.

2.4. Synthesis of WPU Based on Olive Oil-Derived Polyols

The preparation of WPU films was carried out through a multi-stage procedure involving prepolymer formation, chain extension, neutralization, emulsification, and solvent removal.[31, 44] To initiate the synthesis, IPDI, OOP, and DMPA were introduced into a four-necked round-bottom flask equipped with a mechanical stirrer, thermometer, and nitrogen inlet. The formulation was prepared using a molar ratio of 13.5:7.5:3, with the three values corresponding to NCO derived from IPDI, OH derived from OOP, and OH derived from DMPA, respectively. The mixture was stirred at 70°C for 2 hours. After the prepolymer stage, the flask was cooled to ambient temperatures. A solution of the chain extender (VAN-OH, 3 mmol) in tetrahydrofuran (THF) was then added dropwise under constant stirring. This step adjusted the total NCO/OH molar ratio to 1, ensuring a complete reaction among the functional groups. THF was used throughout to reduce viscosity and maintain proper mixing. Following the addition, the reaction was continued at 70°C for an additional 5 hours to complete chain extension. Upon completion of the reaction, the mixture was cooled to room temperature and neutralized by the gradual addition of

triethylamine (TEA). This step was conducted under continuous agitation for 45 minutes to ensure full conversion of the free carboxylic acid groups from DMPA to their corresponding salts. Emulsification was achieved by slowly adding deionized water into the neutralized mixture under vigorous stirring. The dispersion process continued for an additional 30 minutes to form a stable WPU emulsion. Finally, the residual THF solvent was removed under reduced pressure using rotary evaporation. The resulting waterborne polyurethane dispersion was poured into Teflon molds and dried at 30°C to obtain flexible WPU films containing olive oil-derived polyols and VAN-OH as a chain extender (Scheme 1).

2.5. Optimization of Reaction Parameters by DoE Approach

A Design of Experiments (DoE) approach was applied to assess the impact of different variables on the performance of WPU.[45–47] The Taguchi method was used to organize the experimental setup through an orthogonal array based on factorial design. Four main parameters, DMPA, VAN-OH, IPDI, and OOP were identified as key factors affecting WPU properties. Levels for each factor were chosen based on previous studies, and three distinct values were defined for each to allow systematic evaluation, as summarized in Table 1.

Table 1
Different levels of each factor and their corresponding values (screening process parameters).

Factor (gr)	Symbol	Level 1	Level 2	Level 3
Dimethylolpropionic acid	DMPA	0.5	1	1.5
Vanillin diol	VAN-OH	0.5	1	2
Isophorone diisocyanate	IPDI	3	6	9
Olive Oil-Polyols	OOP	8	16	32

Nine experimental runs were conducted using a standard orthogonal array based on the Taguchi design. Minitab software was used for statistical analysis to ensure result accuracy. Each variable was examined at three levels to determine its influence on WPU performance. To further assess the role of VAN-OH as a chain extender, an additional test (Experiment 11) was performed using the same optimized conditions but with VAN-OH omitted (set to zero). This comparison aimed to isolate and evaluate the impact of the chain extender on the final polymer properties. All formulations are listed in Table 2.

2.6. Instrumentation and Characterization Techniques

2.6.1. Particle Size and Distribution

The average particle size and polydispersity index (PDI) of the synthesized WPU emulsions were determined using dynamic light scattering (DLS) on a Brookhaven 90 Plus Laser Particle Analyzer. Prior to measurement, samples were diluted with deionized water to reduce viscosity and ensure accurate light scattering. All analyses were conducted at ambient temperature, and each measurement was

repeated three times to verify reproducibility. The results provided insight into colloidal stability and the effect of formulation parameters on dispersion behavior. This method was essential for evaluating the efficiency of emulsification during synthesis.

2.6.2. Fourier Transform Infrared Spectroscopy (FT-IR)

FT-IR spectroscopy was employed to confirm the chemical structure of the WPU films. Spectra were recorded in attenuated total reflectance (ATR) mode over the wavenumber range of 650–4000 cm^{-1} with a resolution of 8 cm^{-1}. Thin polymer films were placed directly on the ATR crystal for analysis. Characteristic absorption bands corresponding to urethane linkages, carbonyl groups, and hydroxyl functionalities were monitored to confirm successful formation and modifications in the polymer backbone. This analysis enabled the identification of structural differences between various formulations.

2.6.3. NMR Spectroscopy

Proton nuclear magnetic resonance (^1H NMR) and carbon-13 nuclear magnetic resonance (^{13}C NMR) spectra were obtained using a BRUKER DRX-300 AVANCE spectrometer to analyze the chemical structure of olive oil and olive oil-based polyols. These techniques were employed to identify key functional groups and verify the structural changes occurring during the synthesis of polyols. The NMR spectra provided detailed insights into the composition and modifications of both the raw and modified oils. This approach was essential for confirming the successful incorporation of functional groups in the polyol structure.

2.6.4. Contact Angle and Surface Energy

The wettability and surface energy of WPU films were assessed using a DSA30 Contact Angle Goniometer (Krüss GmbH). Contact angle measurements were performed with distilled water and ethylene glycol as probe liquids. Each film was tested at three different spots, and average values were reported. Surface energy was calculated based on the Owens–Wendt method, allowing for the estimation of polar and dispersive components. These parameters helped evaluate the surface characteristics of the films, which are critical for applications such as coatings and adhesives.

2.6.5. Mechanical Properties (Tensile Testing)

The dried WPU films were measured for tensile strength, elongation at break, and Young’s modulus using an Instron 3365 universal testing machine. Testing was conducted at a controlled room temperature of 25°C and a crosshead speed of 50 mm/min, following the ASTM D638 standard. Each sample was tested in triplicate, and the highest value among the replicates was used for comparative analysis. This assessment provided quantitative data on the flexibility and durability of the prepared materials.

2.6.6. Thermal Stability (TGA/DTG)

Thermal properties were analyzed using thermogravimetric analysis (TGA/DTG) on a Pyris instrument. Approximately 7–8 mg of each film sample was placed in a platinum crucible and heated from 25 to

600°C under nitrogen at a rate of 10°C/min. The resulting weight loss curves and derivative peaks were used to determine degradation stages and onset temperatures. This method helped assess the thermal resilience of the WPU and WPU-VAN-OH formulations and the influence of bio-based components on thermal behavior. Comparative analysis between samples provided insight into the relationships between polymer structure and properties.

2.6.7. Surface Morphology (SEM)

The morphological characteristics of WPU and WPU-VAN-OH films were examined using scanning electron microscopy (SEM). Film samples were mounted on aluminum stubs and sputter-coated with a thin layer of gold to improve conductivity. SEM imaging was performed before and after UV curing to investigate structural changes during the curing process. Differences in surface uniformity, porosity, and phase separation were noted. These observations supported other physical and mechanical measurements, offering a visual representation of material integrity and film quality.

2.6.8. Water Absorption Test

Water uptake of WPU and WPU-VAN-OH films was evaluated through immersion tests. Dried films were submerged in deionized water and stored at room temperature for seven consecutive days. Samples were removed daily, blotted to remove surface moisture, and weighed to monitor changes in mass over time. This method provided information on the hydrophilicity and water resistance of the films, which are critical for packaging, biomedical, and coating applications. The influence of formulation parameters, especially chain extender content, was reflected in absorption behavior.

2.6.9. Total Solids Content (TSC)

The total solids content (TSC) of the synthesized dispersions was measured in accordance with ISO 124:1997. One gram of each WPU sample was placed in a pre-weighed crucible and dried in a convection oven at 70°C until a constant weight was achieved. The solid residue was used to calculate TSC as an indicator of dispersion concentration. TSC is crucial in evaluating formulation efficiency and shelf stability.

2.6.10. Stability Evaluation

Stability of the WPU dispersions was assessed by visual inspection over a four-week storage period. Samples were kept in transparent sealed containers at room temperature and monitored for signs of sedimentation, phase separation, or turbidity. A stable dispersion indicated proper emulsification and formulation balance. This qualitative method provided practical insights into storage behavior and product shelf life. Results from this test complemented particle size data and solid content measurements.

2.6.11. Adhesion Tests (Cross-Cut and Pull-Off)

Adhesion strength was examined using cross-cut (ASTM D3359) and pull-off (ASTM D4541) methods. In the cross-cut test, films applied to stainless steel were scored with a multi-blade cutter to form a grid.

Tesa tape was applied and removed to evaluate film retention. For pull-off testing, studs were bonded to cleaned film surfaces using a heat-curable epoxy, and detachment force was measured with a Positest AT-Automatic device. These tests provided quantitative and qualitative data on coating adherence to metallic substrates, essential for protective coating performance.

2.7. Self-Healing Analysis

The self-healing capability of WPU and WPU-VAN-OH films was investigated by making controlled scratches (~ 100 μm depth) on coated mild steel plates using a scalpel.[47] Damaged samples were then subjected to thermal treatment to trigger healing. Pre- and post-healing images were captured using a Zeiss Primostar optical microscope equipped with a 423x AmScope camera. Visual inspection allowed assessment of recovery extent, surface closure, and healing efficiency. During optical microscope observations, the samples were secured to the stage to preserve consistent coordinates. Red circle marks were incorporated into the photos of both WPU and WPU-VAN-OH to distinctly denote the identical scratch area at varying time intervals. The experiment highlighted the effect of formulation components on autonomous repair properties of the films.

2.8. Statistical Analysis

All experimental data were obtained from three independent replicates and are presented as mean values ± standard deviation (SD). All data processing and statistical analyses were carried out using OriginPro 2022 and Minitab Statistical Software (version 22).

Results and Discussion

3.1. Design of Experiments (DoE)

To investigate the factors influencing the mechanical performance of WPU-VAN-OH films, a Taguchi-based experimental design was implemented.[47] This method facilitated the systematic study of variable interactions and their effect on film stress properties.[48] The resulting data were analyzed to identify the most critical factors and determine their optimal levels relative to the target response. The experimental conditions and corresponding factor levels are presented in Table 2.

Table 2
Formulation screening using Taguchi design.

	Factors				**Results**
Test number	DMPA	VAN-OH	IPDI	OOP	Stress [MPa]
1	0.5	0.5	3	8	7.9
2	0.5	1.0	6	16	9.0
3	0.5	2.0	9	32	8.0
4	1.0	0.5	6	32	8.6
5	1.0	1.0	9	8	8.7
6	1.0	2.0	3	16	8.9
7	1.5	0.5	9	16	8.1
8	1.5	1.0	3	32	9.0
9	1.5	2.0	6	8	8.2
10*	1.0	1.0	6	16	9.2
11*	1.0	0.0	6	16	7.5

* Indicates an optimized formulation; all component values are in grams; stress values represent tensile strength in MPa.

The Taguchi analysis indicated that VAN-OH had the greatest influence on the measured response, with 1 g (level 2) determined as the most effective amount. DMPA was identified as the second most significant factor, showing optimal performance at 1 g (level 2). OOP and IPDI followed in order of importance, with optimal levels set at 16 g (level 2) and 6 g (level 2), respectively, based on their effect on film tensile strength. To validate the results, two new formulations Sample 10 and Sample 11 were prepared using the optimized parameter settings. Sample 11 was produced without VAN-OH to serve as a reference, while Sample 10 was used to assess the impact of VAN-OH on polymer characteristics, as illustrated in Fig. 2.

As illustrated in Fig. 3, the tensile strength of the WPU-VAN-OH films reached its highest values when the synthesis parameters were set close to their predicted optimal levels.[49] This trend indicates a strong correlation between formulation variables, particularly VAN-OH, DMPA, OOP, and IPDI, and the mechanical performance of the resulting films. The observed peak in tensile strength suggests that small deviations from the optimized conditions can significantly affect the final properties, highlighting the sensitivity of the system to precise control of reactant ratios. These findings confirm the effectiveness of the statistical model in identifying key parameters that govern film strength and support the importance of optimizing reaction components for enhanced mechanical behavior.

Figure 4 illustrates two-dimensional contour plots generated from the RSM model, depicting the combined effects of synthesis parameters on the tensile strength of WPU-VAN-OH films.[50] The color gradients represent variations in mechanical performance, enabling a clear visual interpretation of optimal and suboptimal regions. As the content of VAN-OH increases to level 2 (1 g), a noticeable enhancement in tensile strength is observed, which can be attributed to improved chain extension and crosslinking density. However, at level 3, the tensile strength decreases, likely due to the excessive amount of chain extender, which promotes an overdevelopment of the hard phase. This, in turn, reduces flexibility, increases brittleness, and causes structural inhomogeneity within the polymer matrix. These results highlight the importance of balanced formulation, where excessive or insufficient levels of VAN-OH can negatively affect film integrity.

Optimizing the DMPA content at level 2 (1.0 g) establishes a balance between polymer chain mobility and matrix cohesion, resulting in improved mechanical strength. The contour plots further indicate a synergistic interaction between VAN-OH and DMPA: while VAN-OH enhances chain extension and flexibility, DMPA introduces carboxylic acid groups that contribute to colloidal stability and structural reinforcement. Together, these components promote higher stress resistance and long-term durability. This combined effect offers a valuable framework for tailoring synthesis conditions to achieve optimal performance in WPU-VAN-OH systems.

3.2. Evaluation of Physicochemical Characteristics of WPU and WPU-VAN-OH

The synthesis of WPU and its VAN-OH-modified counterpart was successfully achieved via a step-growth polymerization mechanism, ensuring the controlled incorporation of functional components into the polymer backbone.[51] As shown in Table 3, distinct differences were observed between the two systems. The unmodified WPU appeared as a milky white emulsion with a total solids content (TSC) of 35%, whereas the WPU-VAN-OH formulation exhibited a pale reddish hue and a slightly higher TSC of 37%. This increase may indicate changes in phase behavior and dispersion stability, potentially influenced by the incorporation of the VAN-OH chain extender and its interaction within the polymer matrix.

The introduction of VAN-OH into the WPU system led to a measurable increase in particle size, as illustrated by the average diameter shifting from 98 nm in unmodified WPU to 109 nm in the WPU-VAN-OH formulation. This increase is consistent with the anticipated rise in molecular weight and chain entanglement introduced by the chain extender, which in turn reduces chain mobility during the emulsification process. Additional formulation parameters such as polyol architecture, NCO/OH ratio, and degree of neutralization also contribute to defining the final particle characteristics. Beyond its role in molecular weight enhancement, VAN-OH influences the colloidal stability of the dispersion. Its molecular structure may introduce both polar and nonpolar functionalities, each exerting distinct effects on dispersion behavior. Polar groups can increase hydrophilicity, potentially promoting flocculation, while hydrophobic segments may induce phase separation or aggregation. Furthermore, elevated viscosity

during the prepolymer stage may impair effective droplet breakup during emulsification, further contributing to larger particle formation. Stability assessments conducted over a four-week period revealed that both dispersions remained colloidally stable during the initial three weeks, with no visible sedimentation and only minor changes in particle size. The WPU system showed a moderate increase in size (from 98 to 136 nm) with a consistently low polydispersity index (PDI ≤ 0.3), indicating stable dispersion. The WPU-VAN-OH formulation exhibited a slightly higher tendency toward aggregation, with particle sizes increasing from 109 to 154 nm and PDI values ranging from 0.2 to 0.32, though it remained visually uniform and functionally stable during this period.

However, by the fourth week, signs of instability became apparent, particularly in the WPU-VAN-OH system, where sedimentation and particle agglomeration were observed. This accelerated destabilization is likely attributed to hydrophobic domains introduced by VAN-OH, which may disrupt colloidal equilibrium over extended storage. While the unmodified WPU exhibited slower degradation kinetics, both systems eventually exceeded the threshold for colloidal stability, underscoring the need for further optimization in formulations intended for long-term storage.

Table 3. The properties of the WPU and WPU-VAN-OH dispersions.

Sample	TSC	Stability			Average Particle size (nm)					
	%	1 week	3 weeks	4 weeks	1 week		3 weeks		4 weeks	
					DLS	PDI	DLS	PDI	DLS	PDI
WPU	35	Stable	Stable	Unstable	98	0.17	136	0.24	----	----
WPU-VAN-OH	37	Stable	Stable	Unstable	109	0.20	154	0.32	----	----

3.3. Characterization of Raw Materials and Polyurethane Films

To investigate the transformation of olive oil into a polyol derivative, we used both ^{1}H and ^{13}C NMR spectroscopy (Figs. 5A,B).[52] This dual technique helped confirm the success of the epoxidation reaction and the subsequent ring-opening, providing a detailed understanding of the structural changes. Starting with raw olive oil, the ^{1}H-NMR spectrum revealed a strong peak around δ 5.3 ppm, which corresponds to the vinylic protons (= CH–CH=) in unsaturated fatty acids like oleic and linoleic acid. Additional peaks were observed at δ 4.1–4.3 ppm, which are attributed to the methylene protons attached to the ester group ($–CH_2–O–$) in the triglyceride structure. The δ 2.0–2.3 ppm region corresponds to the α-protons of the methylene group next to the carbonyl group ($–CH_2–C = O$), while δ 1.2–1.6 ppm and δ 0.9 ppm reflect the presence of methylene and terminal methyl groups, respectively. Following epoxidation, the ^{1}H-NMR spectrum of the polyol derivative showed notable differences. The peak at 5.3 ppm almost disappeared,

signaling the consumption of double bonds in the unsaturated fatty acids. At the same time, new peaks appeared between δ 3.3–3.6 ppm, representing protons attached to hydroxyl groups (–CH–OH and –CH_2–OH), indicating the successful formation of polyol. A corresponding increase in the δ 4.1–4.3 ppm region further suggested the introduction of oxygen-rich functionalities into the structure. For ^{13}C-NMR, the spectrum of raw olive oil displayed distinct carbon signals: δ 172–174 ppm for ester carbonyl groups (C = O), δ 130 ppm for vinylic carbons (C = C), δ 60–70 ppm for the carbons in the glycerol backbone attached to oxygen, and δ 20–40 ppm for the aliphatic methylene and methyl carbons. After epoxidation, the ^{13}C-NMR spectrum of the polyol confirmed the expected structural changes. The 130 ppm peak diminished significantly, indicating the loss of the double bonds. New signals in the δ 60–75 ppm range emerged, attributed to the hydroxyl-bearing carbons in the polyol structure, further confirming the successful transformation. These findings, supported by both ^{1}H and ^{13}C NMR data, clearly show that the epoxidation and ring-opening reaction successfully converted olive oil into a functional polyol derivative, suitable for further modification and use in polymeric applications.

The structural features of the raw materials and final polyurethane films were confirmed by Fourier-transform infrared spectroscopy (FT-IR).[53] The spectrum of DMPA showed a broad absorption around 3353 cm^{-1} corresponding to O–H stretching, while a distinct peak at 1681 cm^{-1} indicated C = O stretching of the carboxylic acid group. In the case of VAN-OH, the formation of imine bonds was evidenced by a signal at 1633 cm^{-1}, while O–H and C–O stretching bands appeared at 3097 and 1028 cm^{-1}, respectively. This confirms the presence of hydroxyl, ether, and imine groups in the VAN-OH molecule. Analysis of the WPU-VAN-OH film revealed well-defined peaks corresponding to the main polymeric functional groups. The strong absorption at 1725 cm^{-1} confirms the presence of urethane C = O bonds, while bands at 1531 and 1413 cm^{-1} are assigned to N–H and C–H bending, respectively. Ether bonds were also confirmed by the 1103 cm^{-1} peak. The broad band centered around 3276 cm^{-1} is attributed to overlapping O–H and N–H stretching vibrations from unreacted hydroxyls and urethane linkages. Importantly, no residual isocyanate (–NCO) peaks were detected in the final polymer spectrum, verifying complete reaction. The presence of imine groups from VAN-OH and the integration of ether and urethane functionalities confirm the successful synthesis of a structurally coherent polyurethane matrix. These spectral results are illustrated in Figs. 5C, D.

3.4. Surface Morphology and Thermal Stability of Polyurethane Films

Scanning electron microscopy (SEM) analysis provided clear evidence of morphological differences between WPU and WPU-VAN-OH films (Fig. 6A, B). The unmodified WPU film exhibited a smooth and homogeneous surface, typical of well-dispersed polyurethane matrices. In contrast, the introduction of VAN-OH led to the development of a visibly rougher surface texture. This surface irregularity can be attributed to increased hydrogen bonding and the formation of additional hard segments in the polymer network. The resulting micro-roughness enhances the film's ability to mechanically interlock with substrates, thus improving adhesion performance. Importantly, this modification did not induce

observable phase separation, indicating that VAN-OH modifies surface characteristics without compromising morphological uniformity.

The thermal degradation characteristics of the synthesized films were examined using TGA and DTG studies (Fig. 6C, D). Both systems commence breakdown at temperatures exceeding 190°C, so affirming their comprehensive thermal resilience. A notable enhancement is shown in WPU–VAN-OH, which maintains its structural integrity more efficiently at elevated temperatures. The improved stability is due to the reinforcing effect of VAN-OH, which fortifies the polymer matrix by enhancing intermolecular connections [54]. The DTG curve for the clean WPU reveals an initial deterioration event commencing at 343°C. This phase is mostly designated for the breakage of urethane bonds, accompanied by the evolution of CO_2. A later degradation phase pertains to the disintegration of OOP parts. For WPU–VAN-OH, both degradation phases occur at elevated temperatures, indicating that the incorporation of aromatic moieties, along with supplementary noncovalent interactions hydrogen bonding and π–π stacking impedes the thermal decomposition process [55]. Nonetheless, the thermal performance of WPU–VAN-OH significantly surpasses that of pristine WPU. This enhancement underscores the efficacy of VAN-OH integration in augmenting thermal resistance, hence broadening the material's application to environments characterized by prolonged high-temperature exposure.

The thermal transitions of the prepared films were further examined using DSC (Fig. 6E). The neat WPU exhibited glass transition events at − 93°C and − 77°C, corresponding to the mobility of soft segments, followed by an endothermic transition at 32°C. Upon incorporation of VAN-OH, these transitions shifted to higher temperatures, with Tg values observed at − 88°C and − 72°C, and a subsequent endothermic peak appearing at 45°C. The upward shift in transition temperatures indicates that VAN-OH incorporation restricts chain mobility and enhances phase stability. This effect is attributed to the presence of aromatic groups and the establishment of additional intermolecular interactions, which reinforce the microphase-separated structure of the polyurethane. Overall, the DSC results confirm that VAN-OH integration improves the thermal response and contributes to enhanced structural rigidity compared with pristine WPU.

3.5. Swelling Behavior

The water absorption behavior of polyurethane films was studied to understand the impact of VAN-OH on moisture resistance over a seven-day period (Fig. 7A).[56] The unmodified WPU film showed a relatively high swelling ratio, beginning at approximately 15% on the first day and increasing steadily to 24.5% by day seven. In contrast, WPU-VAN-OH exhibited significantly reduced swelling, starting at 9% on day one and stabilizing at 14% by the end of the test period. This consistent difference represents a 10% reduction in water uptake across the entire duration.

The reduction in swelling can be attributed to the structural characteristics introduced by VAN-OH. The presence of aromatic rings and Schiff base (C = N) linkages enhances hydrophobicity and restricts the diffusion of water molecules into the polymer matrix. Furthermore, these structural elements promote π–π stacking and strengthen hydrogen bonding within the hard segments, creating a denser and less

permeable network. As a result, the polymer becomes less susceptible to water-induced swelling, which is critical for applications involving exposure to humidity or aqueous environments, such as protective coatings and biomedical films.

3.6. Mechanical Performance

The influence of VAN-OH on the mechanical performance of WPU films was evaluated using stress-strain analysis (Fig. 7B).[57] The results reveal a dramatic increase in tensile strength upon incorporation of VAN-OH. The base WPU film displayed a tensile strength of only 7.5 MPa, whereas the modified WPU-VAN-OH film reached 9.2 MPa nearly a threefold improvement. This substantial enhancement reflects the reinforcing effect of VAN-OH, which increases molecular interactions and introduces rigid aromatic structures into the polymer backbone. This increase in tensile strength was accompanied by a noticeable reduction in flexibility. The elongation at break decreased from 155% in WPU to 113% in WPU-VAN-OH. The decrease in elongation is a direct consequence of the stiffer, more crosslinked network formed by aromatic and imine functionalities in VAN-OH. These segments act as physical crosslinks, restricting polymer chain mobility under tension. Altogether, the integration of VAN-OH not only improves strength but also imparts greater dimensional stability and resistance to deformation. This trade-off between flexibility and strength is often desirable in structural applications, packaging materials, or load-bearing coatings, where toughness and resistance to mechanical stress are prioritized.

3.7. Water Contact Angle and Surface Free Energy

To explore the surface characteristics of the polyurethane films, water contact angle and surface free energy measurements were conducted (Fig. 7C). WPU films exhibited a contact angle of 62.8°, indicating moderate wettability. Upon modification with VAN-OH, the contact angle increased to 69.4°, demonstrating a significant shift toward hydrophobic behavior. In parallel, surface free energy decreased from 41.91 mJ/m² in WPU to 28.15 mJ/m² in WPU-VAN-OH, further confirming the reduced surface polarity.[58] This transformation is primarily due to the presence of aromatic systems and Schiff base linkages in VAN-OH. These structural units introduce rigidity and reduce the overall polarity of the polymer surface. Aromatic rings promote π–π stacking, which leads to a more compact molecular arrangement and limits available polar sites for hydrogen bonding with water molecules. Schiff base linkages also enhance stiffness, further minimizing interaction between the polymer surface and water. The reduction in surface free energy suggests a more thermodynamically stable and less interactive surface, which is advantageous in applications such as anti-fouling coatings, moisture barriers, and electronic encapsulation materials. Hydrophobic surfaces are also beneficial in biomedical applications where water repellency improves performance and stability.

3.8. Adhesion Properties

The adhesive behavior of WPU and WPU-VAN-OH films on stainless steel substrates was examined using both cross-cut and pull-off adhesion tests (Fig. 7D).[59] In the cross-cut test, the unmodified WPU film scored 3B, with approximately 5–15% of the film detaching from the substrate after the tape was pulled off. This result indicates weak adhesion and insufficient interfacial bonding. In contrast, WPU-

VAN-OH achieved a 4B rating, with less than 5% detachment, signifying significantly improved adhesion performance. This improvement is attributed to the enhanced interfacial interactions introduced by VAN-OH. The hydroxyl and aromatic functional groups in VAN-OH promote stronger hydrogen bonding and π–π interactions with the substrate. These interactions increase interfacial compatibility and reduce the likelihood of delamination. Furthermore, the denser and more rigid structure of WPU-VAN-OH improves mechanical interlocking with micro-irregularities on the stainless steel surface, adding a physical dimension to the adhesion enhancement.

The results of the pull-off tensile test aligned with the cross-cut findings. WPU showed an adhesion strength of 12.3 kgf/cm², whereas WPU-VAN-OH exhibited 24.1 kgf/cm² more than a twofold increase. This significant enhancement demonstrates that VAN-OH does not merely improve bulk properties, but also dramatically boosts interface strength, making WPU-VAN-OH highly suitable for demanding coating applications, particularly where strong and durable adhesion to metallic surfaces is required.

3.9. Self-Healing Capability of WPU-VAN-OH Films

Conventional polyurethane coatings typically lack the ability to recover from physical damage such as scratches or cracks, often leading to deterioration in both appearance and performance.[60–62] To overcome this limitation, dynamic covalent bonds particularly imine (Schiff base) linkages have been explored for their reversible nature, enabling materials to autonomously repair structural damage.[63, 64] In this study, the self-healing performance of WPU-VAN-OH films containing dynamic imine bonds was evaluated and compared to that of standard WPU films lacking such functionality (Fig. 8A,b).

The healing experiment was conducted by applying a controlled scratch (approximately 10 μm wide) to the surface of both film types, followed by thermal activation at 80°C. Healing progress was documented using a Zeiss Primostar optical microscope equipped with an AmScope 423x camera at predetermined intervals. In the case of WPU-VAN-OH, the scratch began to contract noticeably after 10 minutes, although the fissure remained partially visible. By the 20-minute mark, the damaged area showed substantial recovery, and complete visual restoration was observed within 30 minutes indicating successful healing of the surface defect. The self-healing behavior of the material is primarily driven by the presence of dynamic imine bonds within the polymer matrix. These bonds can undergo reversible exchange reactions, especially when the material is heated above its glass transition temperature (Tg). At elevated temperatures, increased molecular mobility allows the imine bonds to break and reform through a process known as imine metathesis. In the early stages, local chain movement leads to partial healing of micro-damages. As the process continues, dynamic bond exchange enables the full reconstruction of the disrupted polymer network. During optical microscopy observations, the samples were secured on the microscope stage to guarantee consistent positioning throughout the experiment. Red circular marks were incorporated into the photos of both WPU and WPU-VAN-OH to distinctly indicate the identical scratch location at various time intervals. This mechanism restores the material's surface integrity over time, without requiring any external agents or repair procedures.

In contrast, the unmodified WPU film, lacking dynamic covalent functionality, showed no observable healing under identical conditions. Even after 30 minutes of thermal treatment at 70°C, the scratch remained unchanged, underscoring the importance of incorporating reversible chemical bonds for enabling autonomous repair. These findings emphasize the functional advantage of incorporating vanillin-based chain extenders that introduce imine linkages into the polyurethane network. The resulting WPU-VAN-OH films demonstrate reliable self-healing under mild thermal stimuli, making them promising candidates for advanced coatings where durability, reduced maintenance, and extended service life are essential particularly in harsh or high-wear environments.

The self-healing properties of WPU-VAN-OH stem from the existence of dynamic imine bonds, the concentration of which is contingent upon the amount of VAN-OH used. An increased concentration of VAN-OH would theoretically create more reversible links and accelerate bond exchange; however, it may also disrupt the equilibrium between hard and soft segments, thereby diminishing the overall integrity of the film. In this study, the VAN-OH concentration was established at the optimal level identified using the Taguchi design of experiments, which yielded the most favorable balance of mechanical performance, adhesion, and self-healing efficiency.

Conclusion

The incorporation of vanillin-based diols with dynamic Schiff base linkages into the waterborne polyurethane (WPU) system marks a significant advancement in the development of sustainable, high-performance polymers. This study successfully demonstrated that by leveraging vanillin, a bio-derived and low-cost compound, alongside olive OOP and IPDI, a robust WPU formulation was synthesized, which not only meets the demand for sustainability but also enhances key material properties. The optimized WPU-VAN-OH formulation exhibited a tensile strength of 9.2 MPa, a notable improvement compared to the base WPU formulation, which had a tensile strength of 7.5 MPa. Additionally, the WPU-VAN-OH formulation demonstrated excellent thermal stability, with the onset of degradation at 353°C, indicating its suitability for high-temperature applications. The self-healing capacity of the WPU-VAN-OH formulation was particularly impressive, with complete recovery of surface scratches within 30 minutes at 70°C, showcasing its potential for applications in environments where material integrity is frequently compromised. The inclusion of Schiff base chemistry not only imparted self-healing properties but also provided the material with reprocessability, enabling autonomous repair under mild thermal conditions without the need for external intervention. These performance attributes, combined with the environmentally sustainable composition, position WPU-VAN-OH as a promising candidate for a wide range of applications, including coatings, adhesives, and biomedical devices, where durability, reprocessability, and sustainability are paramount. This work underscores the potential of bio-based polyurethanes to provide innovative solutions to current challenges in material science, offering a pathway for the development of next-generation sustainable polymers.

Declarations

ASSOCIATED CONTENT

No Supporting Information

AUTHOR INFORMATION

Corresponding Author

Ali Reza Banan

E-mail: bananjahromi@yahoo.com

Funding Sources

No funding to declare.

Data Availability

Data is provided within the manuscript files.

ACKNOWLEDGMENT

This work was supported by department of organic chemistry, Imam Hossein University

References

1. Mayer A (2022) Energy Sustain Soc 12:27
2. Hosseini SE (2022) Future Energy 1:2–5
3. Wang J, Azam W (2024) Geosci Front 15:101757
4. Siddik M, Islam M, Zaman A, Hasan M (2021) Int J Energy Environ Econ 28:103–119
5. Alola AA, Adebayo TS (2023) Sci Total Environ 887:164115
6. Bianchini VK, do Amaral Razzino C, Pakes PR, Bianchini GF (2024) A. G. A. Filho and A. L. V. Torkomian
7. Zhou X, Sun Z, Yan H, Feng X, Zhao H, Liu Y, Chen X, Yang C (2021) J Clean Prod 308:127283
8. Abed J, Rayburg S, Rodwell J, Neave M (2022) Sustainability 14:5570
9. Singh N, Ogunseitan OA, Wong MH, Tang Y (2022) Sustainable horizons 2:100016
10. Bodachivska LY (2021) Catal petrochemistry, 55–61
11. Chin SY, Shahruddin S, Chua GK, Samsodin N, Setiabudi HD, Karam Chand NS, Chew FN, Leong JX, Jusoh R, Samsudin NA (2021) ACS Sustain Chem Eng 9:6510–6533
12. Rajendran S, Al-Samydai A, Palani G, Trilaksana H, Sathish T, Giri J, Saravanan R, Lalvani JIJ, Nasri F (2025) Eng Rep 7:e70108
13. Gharby S (2022) *The Scientific World Journal*, 2022, 6627013
14. Machado M, Rodriguez-Alcalá LM, Gomes AM, Pintado M (2023) Food Reviews Int 39:4180–4197

15. Cui M, Chai Z, Lu Y, Zhu J, Chen J (2023) Resour Chemicals Mater 2:262–276
16. De Souza FM, Kahol PK, Gupta RK (2021) Polyurethane chemistry: Renewable polyols and isocyanates. ACS, pp 1–24
17. Wienen D, Gries T, Cooper SL, Heath DE (2023) J Controlled Release 363:376–388
18. Jiang R, Zheng X, Zhu S, Li W, Zhang H, Liu Z, Zhou X (2023) ChemistrySelect 8:e202204132
19. Li Y, Zhou M, Wang R, Han H, Huang Z, Wang J (2024) Eur Polym J 214:113159
20. Kim S, Li K, Alsbaiee A, Brutman JP, Dichtel WR (2023) Adv Mater 35:2305387
21. Hao M, Li X, Zhong Y, Zhang B, Wang F (2021) J Mater Civ Eng 33:04020485
22. Bratasyuk NA, Ostanin SA, Mokeev MV, Zuev VV (2022) Polym Adv Technol 33:3173–3191
23. Jiang S, Wong JS, Puhan D, Yuan T, Bai X, Yuan C (2024) Friction 12:1801–1815
24. Zhao L, Hong C, Wang C, Li J, Ren H, Zhou C (2023) Prog Org Coat 183:107765
25. Gonçalves M, Vale N, Silva P (2024) Antioxidants 13:762
26. Afonso IS, Cardoso B, Nobrega G, Minas G, Ribeiro JE, Lima RA (2024) J Environ Chem Eng 12:114022
27. Tsimihodimos V, Psoma O (2024) Int J Mol Sci 25:8117
28. Hashempour-baltork F, Zade SV, Mazaheri Y, Alizadeh AM, Rastegar H, Abdian Z, Torbati M, Damirchi SA (2024) J Agric Food Res 16:101123
29. Sumathi S, Shakina J, Tharmaraj P (2025) J Polym Res 32:227
30. Salarvand E, Omrani I (2024) and M. Salehi
31. Mucci VL, Hormaiztegui M (2020) and M. I. Aranguren
32. Miller LJ, Sawyer-Beaulieu S, Tam E (2014) SAE Int J Mater Manuf 7:711–718
33. Miravalle E, Bracco P, Brunella V, Barolo C, Zanetti M (2023) Polymers 15:3780
34. Li Q, Ma S, Li P, Wang B, Feng H, Lu N, Wang S, Liu Y, Xu X, Zhu J (2021) Macromolecules 54:1742–1753
35. Li X, Zhang T, Song B, Yang K, Hao X, Ma J (2024) J Appl Polym Sci 141:e54762
36. Zhao X-L, Zhang Z-W, Li Y-D, Du A-K, Wu Y, Zeng J-B (2023) ACS Sustain Chem Eng 11:9846–9857
37. Schoustra SK, Groeneveld T, Smulders MM (2021) Polym Chem 12:1635–1642
38. Moon HH, Cha I, Hegazy HA, Song C (2023) Bull Korean Chem Soc 44:750–767
39. Patil DG, Magdum PA, Nandibewoor ST (2015) J Solut Chem 44:1205–1223
40. Rashid MA, Liu W, Wei Y, Jiang Q (2022) Polymer-Plastics Technol Mater 61:1740–1782
41. Caillol S, Desroches M, Boutevin G, Loubat C, Auvergne R, Boutevin B (2012) Eur J Lipid Sci Technol 114:1447–1459
42. Alagi P, Choi YJ, Hong SC (2016) Eur Polym J 78:46–60
43. Kaikade DS, Sabnis AS (2023) Polym Bull 80:2239–2261
44. Calovi M, Rossi S (2023) Coatings 13:442

45. Nezadi M, Keshvari H, Yousefzadeh M (2021) Adv nano Res 10:59–69
46. Selvaraj VK, Subramanian J, Krishna Rajeev P, Rajendran V, Raja S (2025) Polym Eng Sci 65:14–28
47. Banan AR (2025) Sci Rep 15:21844
48. Tamsilian Y, Babadi MA, Zalakinezhad A, Savaedi SA, Jamalpour S (2024) Colloids Surf A 690:133728
49. Garg N, Rastogi V, Kumar P (2022) *Materials Today: Proceedings*, 62, 94–99
50. Al-Kahtani M, Zhu H, Ibrahim YE, Haruna S, Al-Qahtani S (2023) Appl Sci 13:13348
51. Gharrak AE, Essamlali Y, Amadine O, Aboulhrouz S, Hafnaoui A, Ghalfi H, Zahouily M (2022) Prog Org Coat 170:106982
52. Barszczewska-Rybarek I, Jaszcz K, Chladek G, Grabowska P, Okseniuk A, Szpot M, Zawadzka M, Sokołowska A, Tarkiewicz A (2022) Polym Bull 79:3061–3083
53. Thiyagu C, Manjubala I, Narendrakumar U (2021) *Materials Today: Proceedings*, 45, 3982–3985
54. Yang W, Lu B, Puglia D, Niu D, Xu P, Ma P (2024) Macromolecules 58:526–537
55. Xu B, Yin Q, Han F, Cheng J, Zhao J, Zhang J (2022) Chem Eng Sci 258:117736
56. Tanasić J, Erceg T, Tanasić L, Baloš S, Klisurić O, Ristić I (2021) React Funct Polym 169:105085
57. Dong H, Li H, Yang Z, Shi H, Li L, Huang F, Wen J (2024) J Building Eng 98:111357
58. Jiang Y, Wang C, Liu M, Gu B, Wang X, Xu C, Xiao G, Miao D, Du J (2024) J Appl Polym Sci 141:e55434
59. Brzozowska K, Chowaniec-Michalak A (2023) P. Niewiadomski and Ł. Sadowski
60. Wei K, Cao X, Wu Y, Tang B, Shan B, Zhang X (2025) J Clean Prod 500:145291
61. Zhang Y, Liu R, Wu Z, Lyu B, Liu L (2024) ACS Sustain Chem Eng 12:16834–16846
62. Du R, Zhou G, Wang X (2025) Macromol Chem Phys 226:2400493
63. Chen K, Zhu H, Zhang Z, Shao Y, Yu Q, Cao X, Pan S, Mu X, Gao Z, Wang D (2023) Chem Eng J 474:145811
64. Hao Q, Huang Y, Chen H, Liu J, Liu J, Xin Z, Bao C (2025) ACS Appl Polym Mater

Scheme 1

Scheme 1 is available in the Supplementary Files section.

Figures

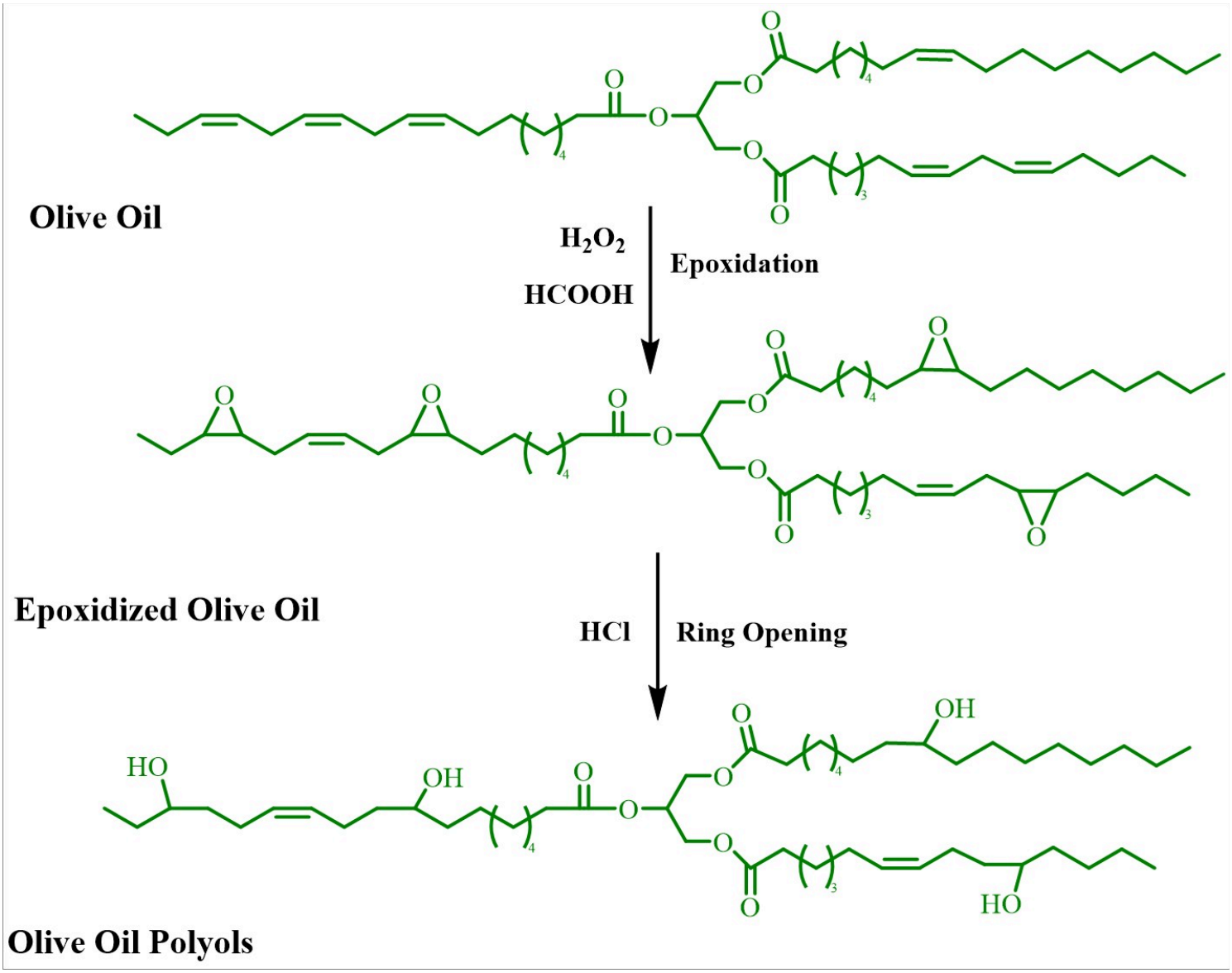


Figure 1

Schematic representation of the synthesis pathway of olive oil-based polyols, involving epoxidation of the double bonds and a subsequent ring-opening reaction.

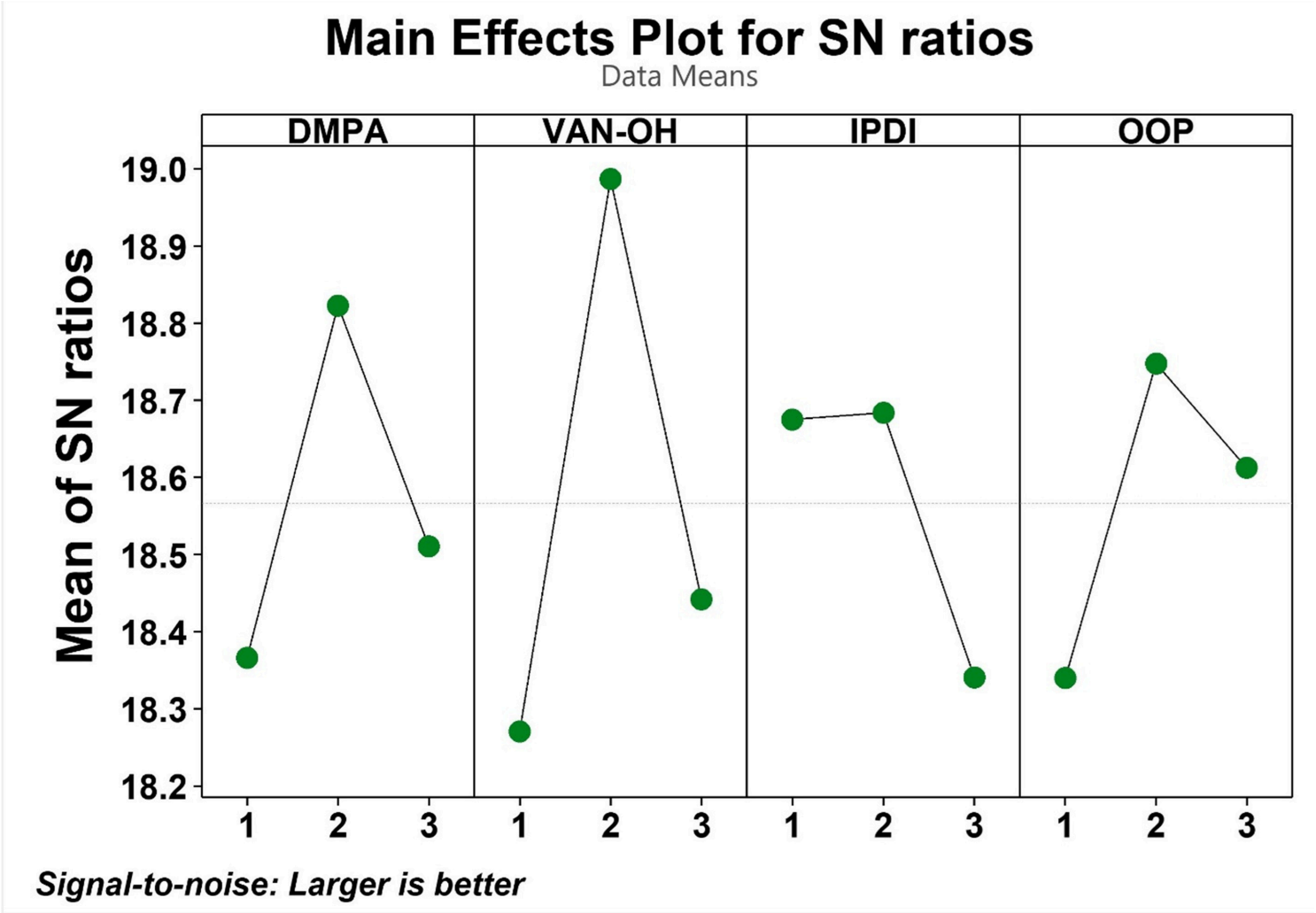


Figure 2

Signal-to-noise ratio curves for determining the optimal factor values.

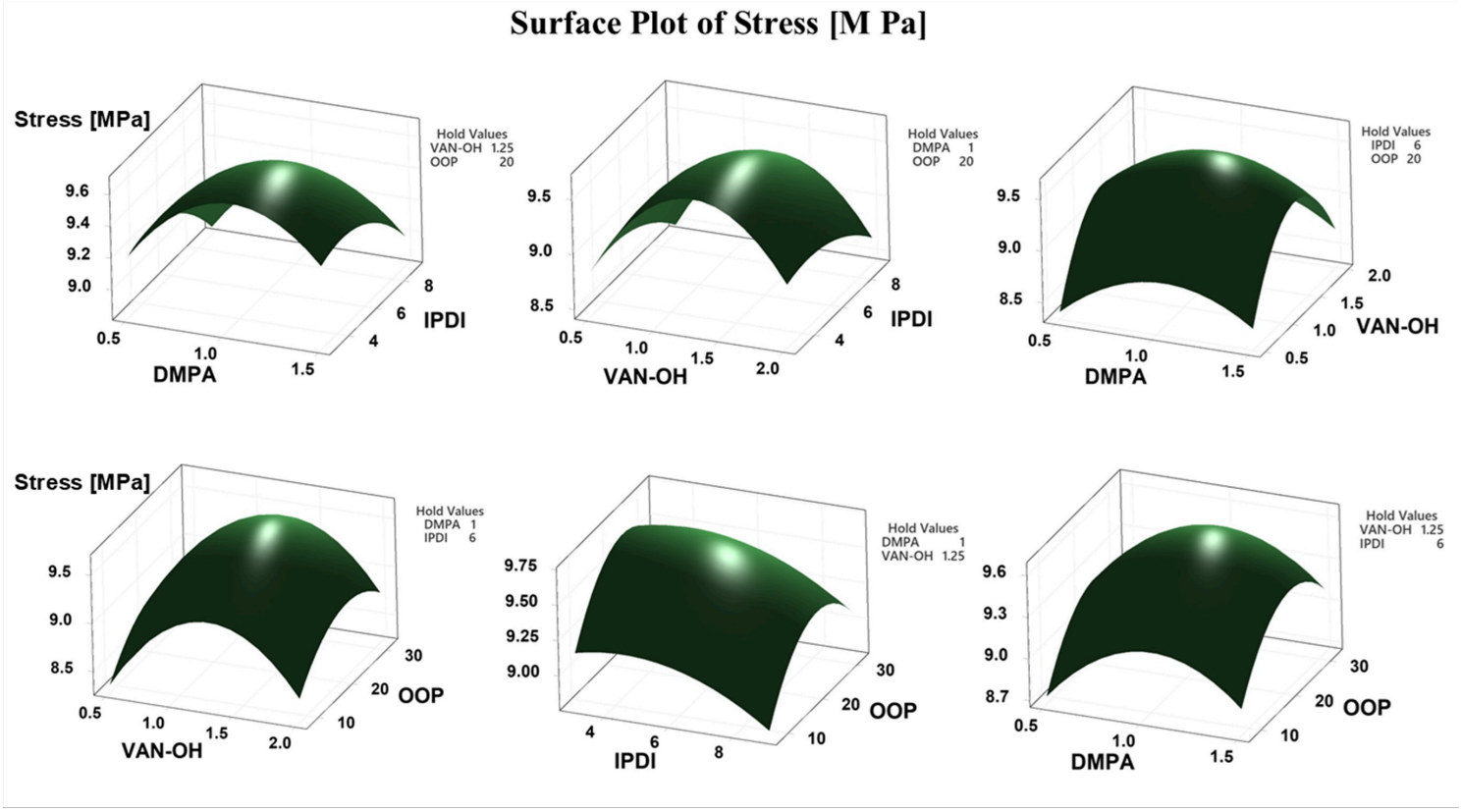


Figure 3

3D surface plot of the response surface model shows the influence of two factors on the tensile strength of the WPU-VAN-OH film.

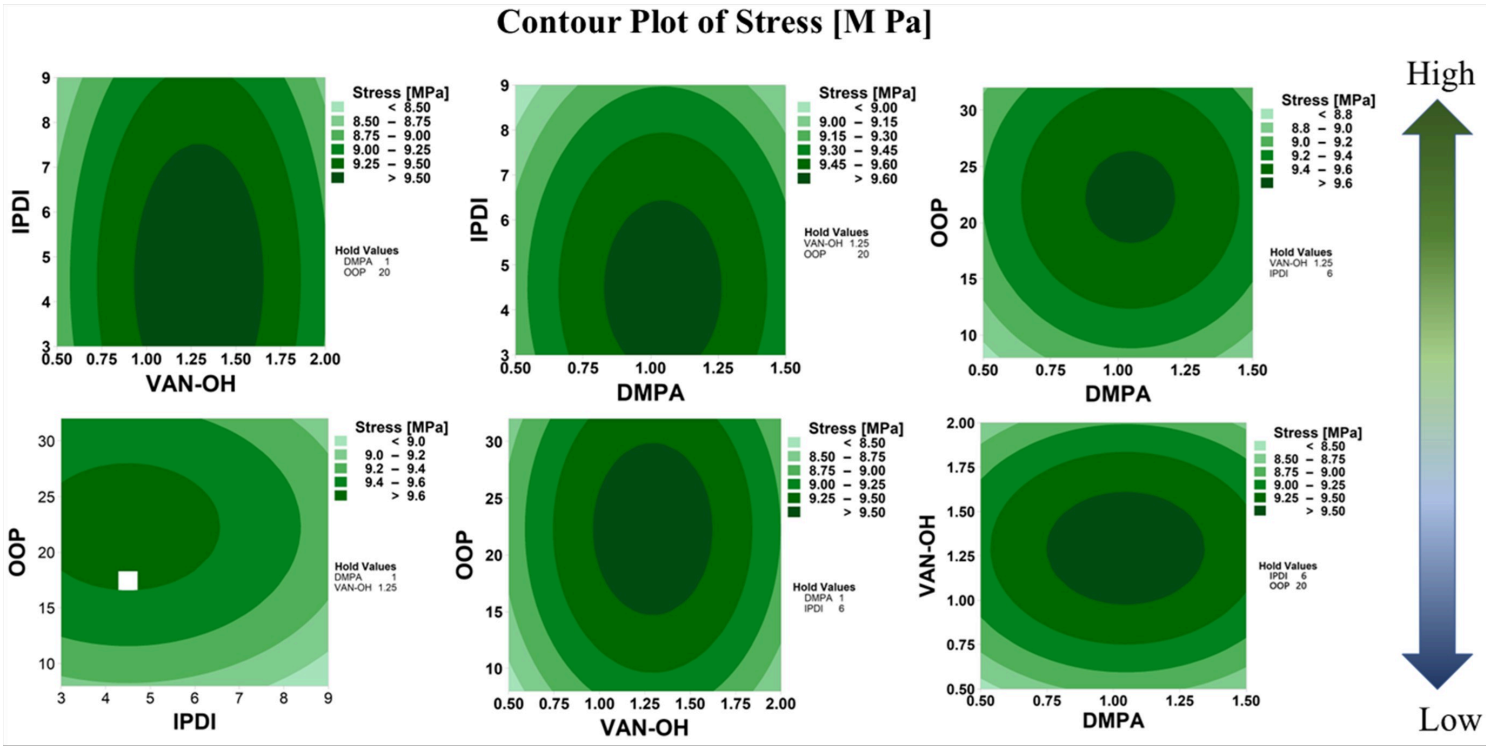


Figure 4

Response surface model contour plot illustrating the impact of two factors on the tensile strength of the WPU-VAN-OH film.

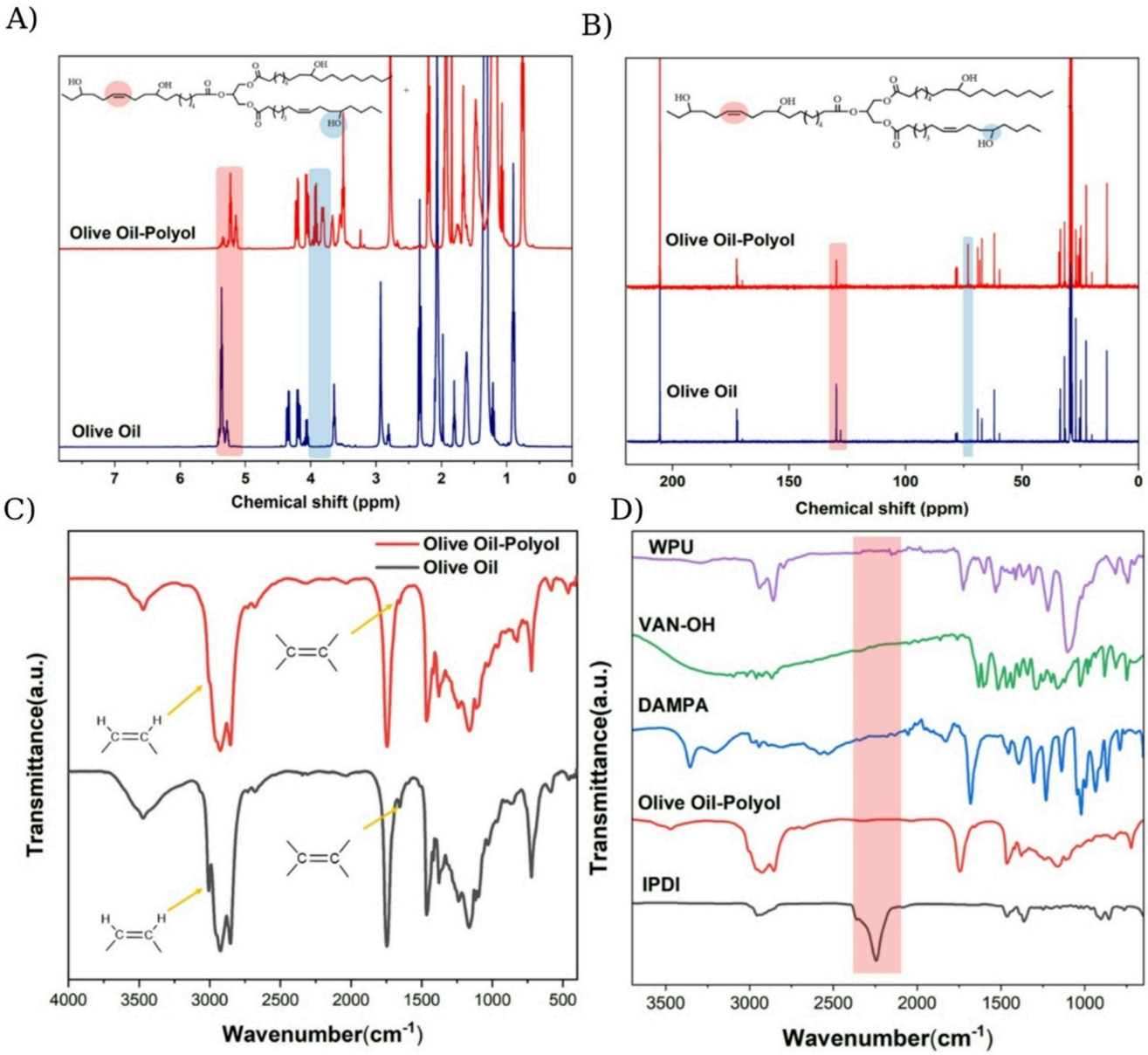


Figure 5

Characterization of WPU, WPU-VAN-OH, and OOP: (A, B) ^{1}H-NMR and ^{13}C-NMR spectra of OO and OOP. (C) FT-IR spectra of OO and OOP. (D) FT-IR spectra of the WPU-VAN-OH film.

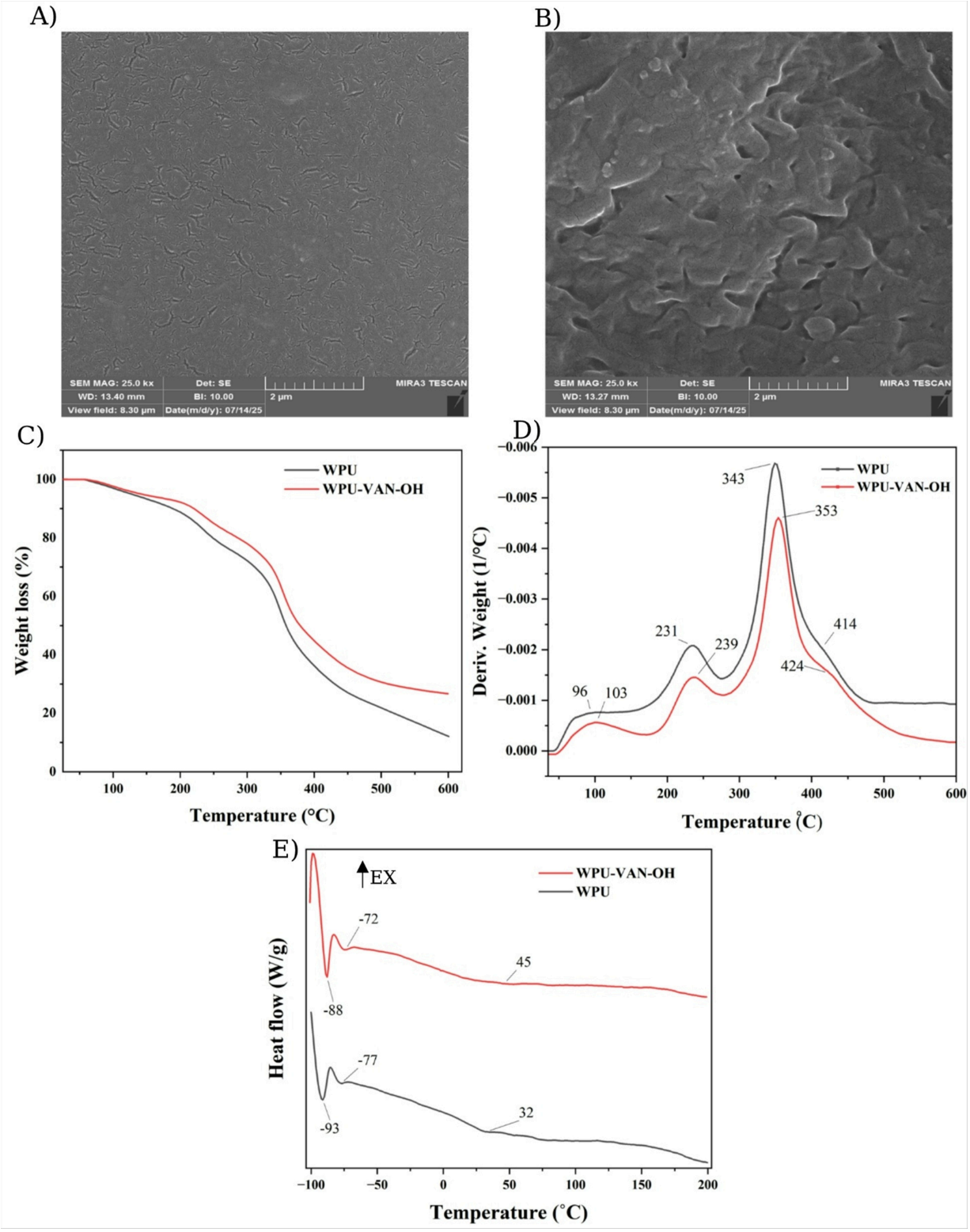


Figure 6

(A, B) SEM micrographs illustrating the surface morphology of WPU and WPU–VAN-OH films. (C) TGA and (D) DTG curves demonstrating the thermal degradation behavior of the films. (E) DSC thermograms highlighting the thermal transitions of WPU and WPU–VAN-OH.

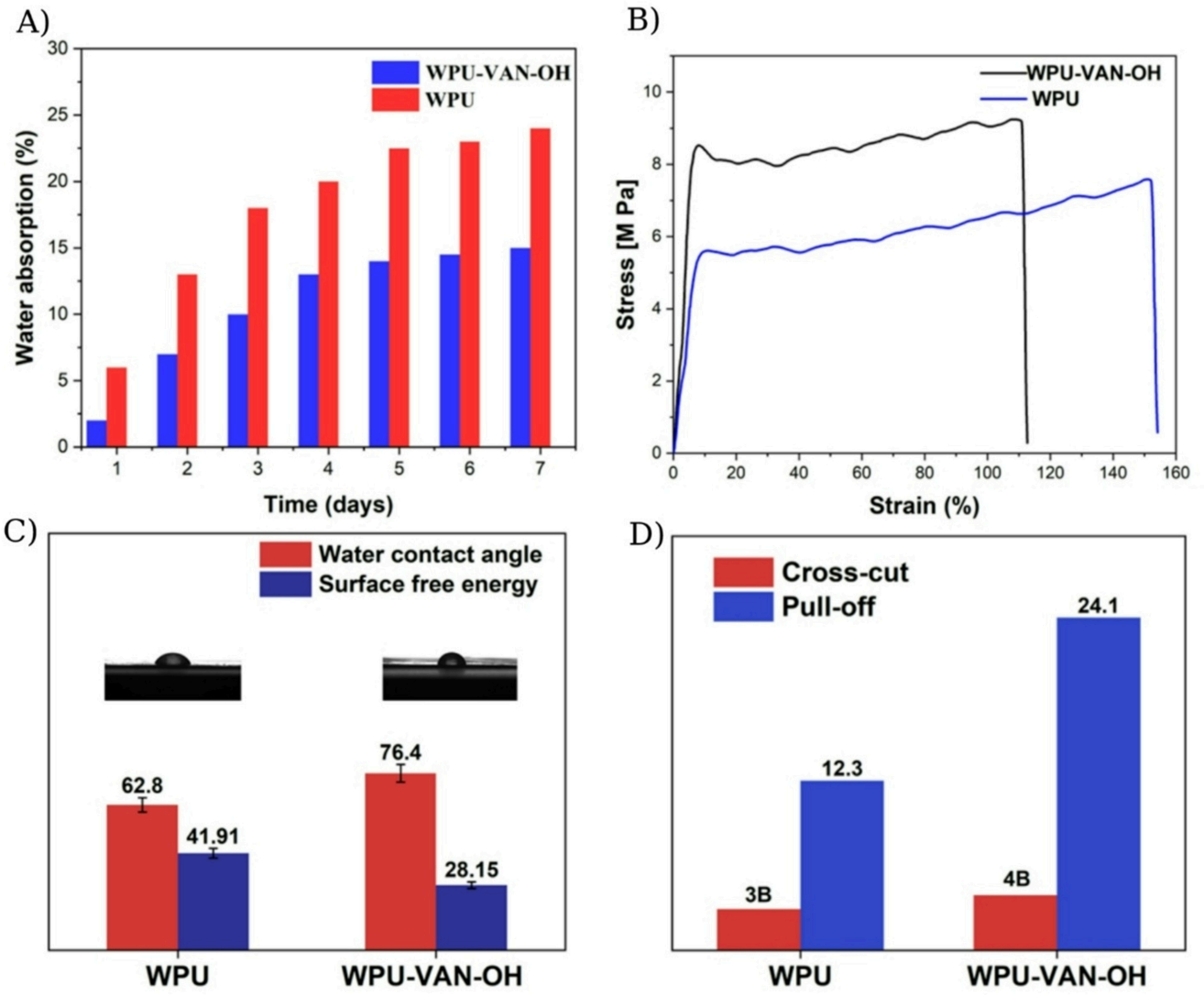


Figure 7

Comparative study of WPU and WPU-VAN-OH films: (A) Water absorption; (B) Mechanical performance (stress–strain behavior); (C) Water contact angle and surface free energy; (D) Adhesion strength (cross-cut and pull-off tests).

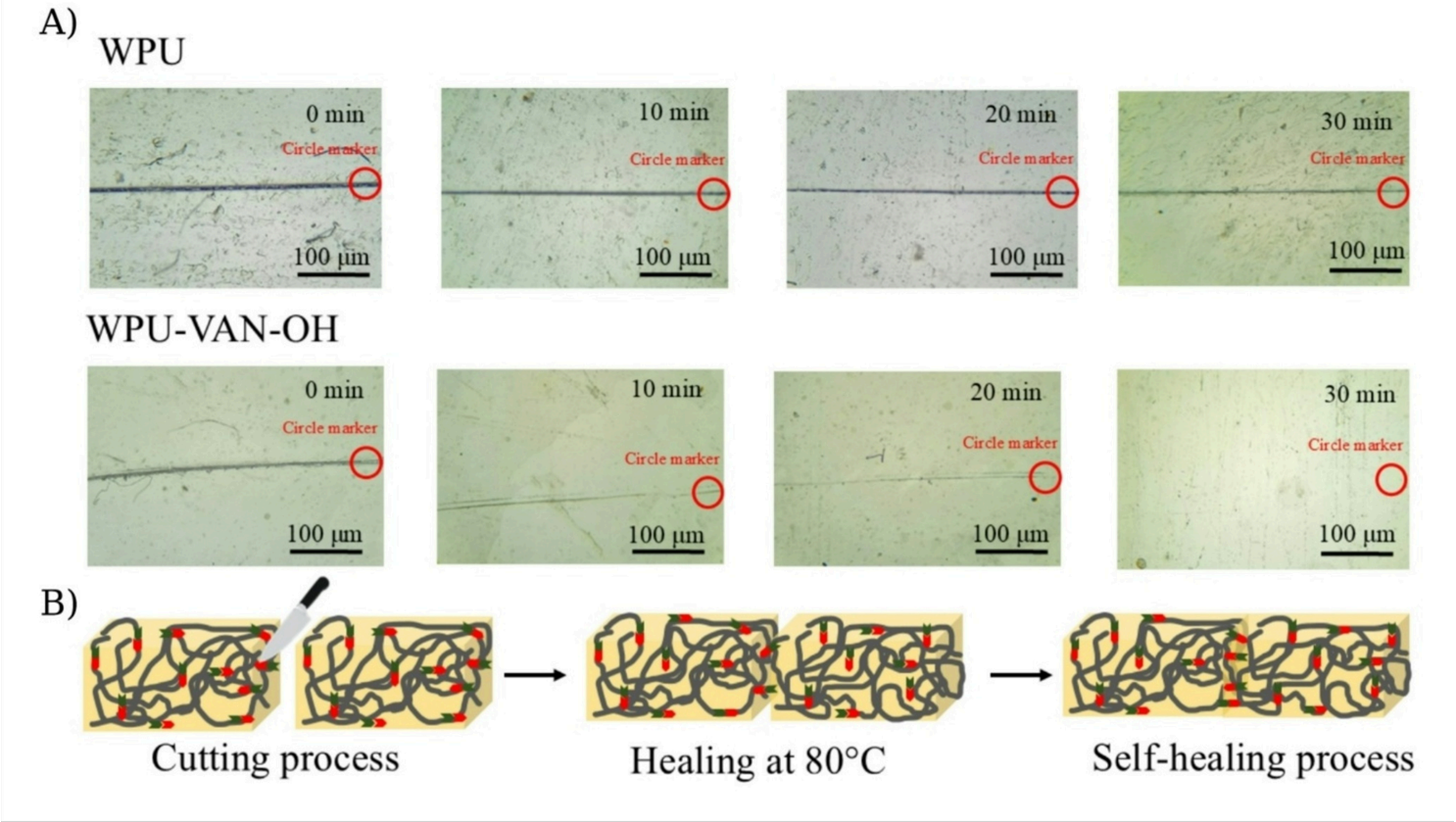


Figure 8

(A) Optical microscopy images of a scratched pristine sample before and after healing at 70°C, captured at different time intervals. (B) Schematic illustration of the self-healing mechanism driven by the imine metathesis reaction. Red circles indicate the same scratch location throughout the healing process

Supplementary Files

This is a list of supplementary files associated with this preprint. Click to download.

- floatimage2.png